Basins of Attraction and Transient Chaos in a Gear-Rattling Model

Silvio L.T. de Souza and Iberê L. Caldas

Journal of Vibration and Control 2001 7: 849
DOI: 10.1177/107754630100700605

Basins of Attraction and Transient Chaos in a Gear-Rattling Model

SILVIO L. T. de SOUZA
IBERÊ L. CALDAS
Institute of Physics, University of São Paulo, C. P. 66318, 05315-970, São Paulo, SP, Brazil

(Received 31 May 2000; accepted 3 November 2000)

Abstract: The authors numerically investigate basins of attraction of coexisting periodic and chaotic attractors in a gear-rattling impact model. These attractors are strongly dependent on small changes of the initial conditions. Gradually varying a control parameter, the size of these basins of attraction is modified by global bifurcations of their boundaries. Moreover, the topology of these basins is also modified by appearance or disappearance of coexisting attractors. Furthermore, for the considered control parameter range, the fractal basin boundaries are so interleaved that trajectories are practically unpredictable in some regions of phase space. The authors also examine an example of a crisis on which a chaotic attractor is converted into a chaotic transient that goes to a periodic attractor. For this crisis, the authors show the evolution of transient lifetime dependence of the initial conditions as the control parameter is varied.

Key Words: Gear-rattling, impact, basins of attraction, transient chaos

1. INTRODUCTION

Mechanical systems exhibiting impacts have been the subject of growing interest in the engineering literature (Moon, 1998). These systems arise whenever their components collide with each other or with rigid obstacles, and they are called *impact oscillators* (or vibro-impact systems). Since these oscillators do not satisfy the usual smoothness assumptions, classical mathematical methods are applicable only to a limited extent and require extensions both for analytical and numerical methods (Moon, 1998; Thompson, 1996).

The gearbox with rattling vibrations is one important type of impact oscillator, rattling being a consequence of backlashes and an unwanted comfort problem in automobiles (Pfeiffer, 1988; Pfeiffer and Kunert, 1990). General models have been developed to analyze these rattling phenomena and find a way of reducing rattling by parameter variation (Karagiannis and Pfeiffer, 1991). Thus, several complex dynamical phenomena induced by the presence of discontinuities in these systems have been reported (Hinrichs, Oestreich, and Popp, 1997; Okolewska and Peterka, 1998; Win et al., 1995; Kaharaman and Singh, 1990; Li, Rand, and Moon, 1990; Nordmark, 1991; Peterka and Vacik, 1992; Casas et al., 1996). However, additional studies are necessary to understand the dynamics of these oscillators, as their rich bifurcations or their significant dependence on control parameters.

Journal of Vibration and Control, 7: 849-862, 2001

Here, we consider two coupled gears described by a gear-rattling deterministic model with impacts (Karagiannis and Pfeiffer, 1991). The motion of one gear is given by a harmonic function while the motion of the other is governed by the dynamics, namely, it is composed by a solution of a differential equation, between two impacts, interrupted by a sequence of impacts. In addition, this nonsmooth dynamical system has one degree of freedom with harmonic external excitation. In engineering, it is common to look for linear stable steady-state oscillations, often by approximate analytical averaging or perturbation methods. However, a nonlinear basin analysis is also necessary to ensure that there is a good sizeable robust basin around the attractor of interest (Thompson, 1996; Grebogi, Ott, and Yorke, 1987). This is especially important for systems with evidences of fractal basin boundaries, like the one we are considering here. For this system, it is also important to study the basin of attraction of transient motions and their dependence on the control parameters (Thompson, 1996; Grebogi, Ott, and Yorke, 1983).

In this work, we investigate numerically the coexistence of multiple (periodic and chaotic) attractors, for fixed sets of values of control parameters, in the described gear-rattling model. We also determine their basins of attraction (Grebogi, Ott, and Yorke, 1983; Nusse and Yorke, 2000), that is, the set of all initial conditions for which the trajectories asymptotically approach a particular attractor. We find regions of phase space with interleaved fractal basin boundaries. Knowledge of these basins and its boundaries supplies important information allowing a prediction of the long-term behavior of the system. Moreover, we show how variations of a control parameter modify the attractors and their basins.

We also investigate chaotic transients of observed attractors. As a control parameter (the amplitude excitation) is gradually increased, we find that chaotic attractors are destroyed and replaced by periodic attractors with long chaotic transients as in crises observed for two-dimensional maps (Grebogi, Ott, and Yorke, 1983). Fixing the control parameter value, we also calculate the chaotic transient lifetime for sets of initial conditions in a grid of points in a section of the three-dimensional phase space. This analysis reveals that the transient lifetime is not uniform for the considered initial conditions. In fact, there are continuous regions of initial conditions where this transient is very short and others with interleaved small regions of very short or very long transients. Near the critical parameter value of the crisis, as the control parameter increases, the interleaved long transient regions decrease, decreasing also the average lifetime.

In Section 2, we describe the gear-rattling system investigated in this work and present the mathematical description of the considered system and its dynamical analysis. In Section 3, we present numerical results of basins of attraction. In Section 4, we discuss the dynamics of the system, present numerical results concerning the observed chaotic transients, and analyze the transient lifetime dependence on the initial conditions and on the control parameter. Finally, in Section 5 we summarize and discuss our main conclusions.

2. MATHEMATICAL DESCRIPTION AND DYNAMICAL ANALYSIS

Figure 1 shows a schematic diagram of the impact mechanical system (Karagiannis and Pfeiffer, 1991). The system is composed of two gears with a backlash v between the teeth. The motion of one gear is given by a harmonic function, while the motion of the other gear is

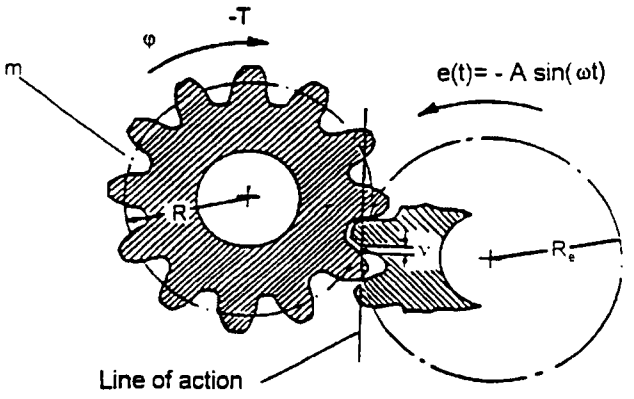

Figure 1. Model of gearbox system.

a combination of a smooth motion governed by a linear differential equation interrupted by a series of nonsmooth impacts.

The smooth motion in the absolute coordinate system is described by the equation

$$m\ddot{\varphi} + d\dot{\varphi} = -T, \tag{1}$$

where m, d, and T are the moment of inertia, damping, and torque, respectively.

The relative displacement S in backlash is given by

$$S(\varphi, t) = AR_e \sin(\omega t) - R\varphi, \tag{2}$$

where R_e and R are the radius of the gears.

Substituting equation (2) into equation (1) and introducing the variable $s = S/v$, the equation of motion in relative coordinates is

$$\ddot{s} + \beta\dot{s} = \ddot{e} + \beta\dot{e} + \gamma \quad \text{for} \quad -1 < s < 0, \tag{3}$$

with $e = -\alpha \sin(\omega t), \dot{s} \equiv \dfrac{ds}{d\tau}$, and $\tau = \omega t$, where $\beta \equiv d/(m\omega), \gamma \equiv (TR)/(m\omega^2), \alpha \equiv AR_e/v$ are damping, moment, and excitation amplitude, respectively.

Integrating equation (3) and invoking initial condition $(s(\tau_0) = s_0, \dot{s}(\tau_0) = \dot{s}_0)$, the displacement s and velocity $\dot{s}$ between impacts are

$$\begin{aligned} s &= s_0 + \alpha[\sin(\tau) - \sin(\tau_0)] + \frac{\gamma}{\beta}(\tau - \tau_0) \\ &+ \frac{1}{\beta}\{1 - \exp[-\beta(\tau - \tau_0)]\}\left[\dot{s}_0 - \alpha\cos(\tau_0) - \frac{\gamma}{\beta}\right] \end{aligned} \tag{4}$$

$$\dot{s} = \alpha \cos(\tau) + \left[\dot{s}_0 - \alpha \cos(\tau_0) - \frac{\gamma}{\beta}\right] \exp\left[-\beta(\tau - \tau_0)\right] + \frac{\gamma}{\beta}. \tag{5}$$

An impact occurs wherever $s = -1$ or 0 (backlash boundaries). After each impact, we apply the Newton law of impact into equations (4) and (5). The new set of initial conditions is

$$\begin{aligned} \tau_0 &= \tau \\ s_0 &= s \\ \dot{s}_0 &= -r\dot{s}, \end{aligned} \tag{6}$$

where r is a constant coefficient of restitution.

Therefore, the dynamics of the gear-rattling system is governed by equations (4), (5), and (6). From these equations, in our numerical simulations we observe both periodic and chaotic attractors.

To analyze the attractors found in numerical simulations, we use an impact mapping, that is, for each impact n (at $s = -1$ or 0), the variables s_n, $\dot{s}_n$, and $\tau_n \pmod{2\pi}$ are computed. These variables correspond to the dynamical variables $s, \dot{s}$, and τ just before the impact.

We characterize the attractors by their Lyapunov exponents. To calculate these exponents for the gear-rattling nonsmooth system, we use a transcendental map as the following. The variables s_{n+1}, $\dot{s}_{n+1}$, and τ_{n+1} are obtained from equations (4) and (5) for the initial conditions

$$\begin{aligned} \tau_0 &= \tau_n \\ s_0 &= s_n \\ \dot{s}_0 &= -r\dot{s}_n. \end{aligned} \tag{7}$$

Thus, we introduce the transcendental map (obtained from equations (4), (5), and (7)):

$$\begin{aligned} s_{n+1} &= s_n + \alpha\left[\sin(\tau_{n+1}) - \sin(\tau_n)\right] + \frac{\gamma}{\beta}(\tau_{n+1} - \tau_n) \\ &\quad - \frac{1}{\beta}\left\{1 - \exp\left[-\beta(\tau_{n+1} - \tau_n)\right]\right\}\left[r\dot{s}_n + \alpha\cos(\tau_n) + \frac{\gamma}{\beta}\right] \\ \dot{s}_{n+1} &= \alpha\cos(\tau_{n+1}) - \left[r\dot{s}_n + \alpha\cos(\tau_n) + \frac{\gamma}{\beta}\right]\exp\left[-\beta(\tau_{n+1} - \tau_n)\right] + \frac{\gamma}{\beta}. \end{aligned} \tag{8}$$

Using the transcendental map (8), we develop an algorithm for the determination of the Lyapunov exponents. To use this algorithm, we first evaluate the Jacobian (for $s_n = -1$ or 0)

$$D_n = \begin{pmatrix} \frac{\partial \tau_{n+1}}{\partial \tau_n} & \frac{\partial \tau_{n+1}}{\partial \dot{s}_n} \\ \frac{\partial \dot{s}_{n+1}}{\partial \tau_n} & \frac{\partial \dot{s}_{n+1}}{\partial \dot{s}_n} \end{pmatrix}, \tag{9}$$

with the eigenvalues $\Lambda_i(n)$ of

$$M = D_n D_{n-1} \ldots D_1. \tag{10}$$

Then, the Lyapunov exponents can be expressed by

$$\lambda_i = \lim_{n \to \infty} \frac{1}{n} \ln |\Lambda_i(n)|, \quad i = 1, 2. \tag{11}$$

3. BASINS OF ATTRACTION

In this section we study attractors of the gear-rattling model, described in the previous section, and how they change as a parameter control is varied. Thus, we numerically calculate trajectories, attractors, bifurcation diagrams, and basins of attraction of these attractors. We choose the excitation amplitude, α, as the control parameter. The results presented are obtained by varying α gradually in the range [0.47, 0.60] and fixing the other system parameters in the usual following values $\beta = 0.10, \gamma = 0.10$, and $r = 0.90$. We discard several thousand iterates to ensure that the transient has died away.

Figure 2 shows a bifurcation diagram of the system, namely, the relative velocity just before each impact, $\dot{s}_n$, as a function of the excitation amplitude, α. The bifurcation diagram is obtained choosing different initial conditions at each α. For each initial condition, we first neglect a sufficiently large number of iterations to get rid of the transient, then plot the subsequent few hundred iterates. As indicated in this figure, we identify three different coexisting attractors. One attractor, A, for the whole bifurcation parameter range, another attractor, B, is present for almost the whole parameter range, and a third attractor, C, is observed only for a shorter variation of this parameter.

In the bifurcation diagram, we recognize mostly periodic motion but also sequences of period doubling bifurcations to chaos and crisis leading to sudden expansions of the chaotic attractor B for large α. The dominant attractors are A and B. Attractor A is periodic in the whole parameter range. Increasing the parameter α, attractor B (initially periodic) undergoes a sequence of period-doubling bifurcations to chaos. After that, there is a transformation from a four-piece to a two-piece attractor, as the parameter passes through a critical value. At another critical parameter, there is a sudden attractor increase as the two-piece attractor merges into a single piece. Finally, attractor B disappears at the end of the considered parameter variation. The third attractor C is suddenly created and destroyed, suffering period-doubling bifurcations to chaos.

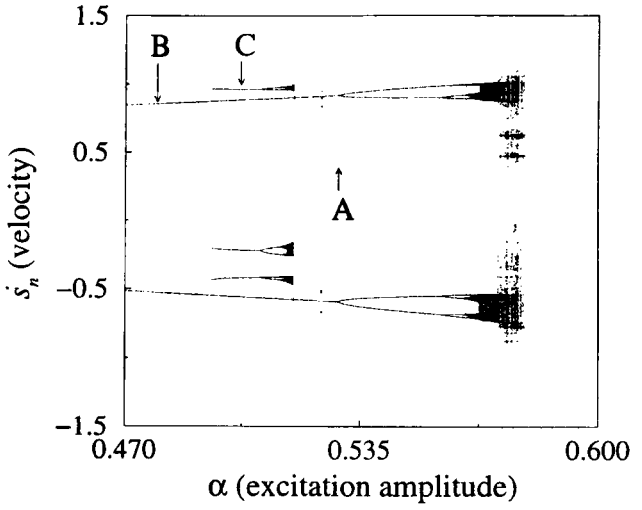

Figure 2. Bifurcation diagram of the velocity $\dot{s}_n$ just before impact as a function of the excitation amplitude α.

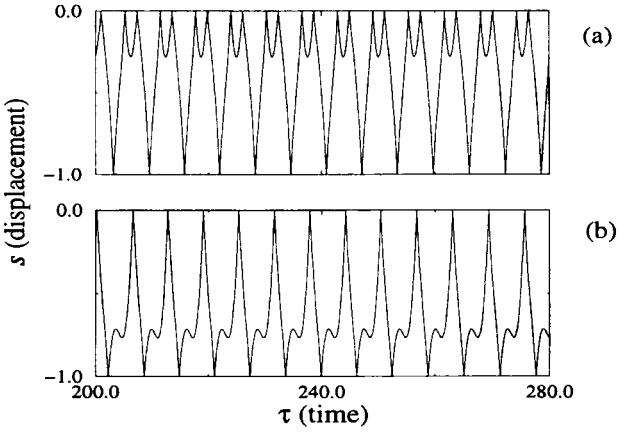

Figure 3. Displacement s as a function of time for the two coexisting periodic attractors A (a) and B (b). Control parameter $\alpha = 0.48$.

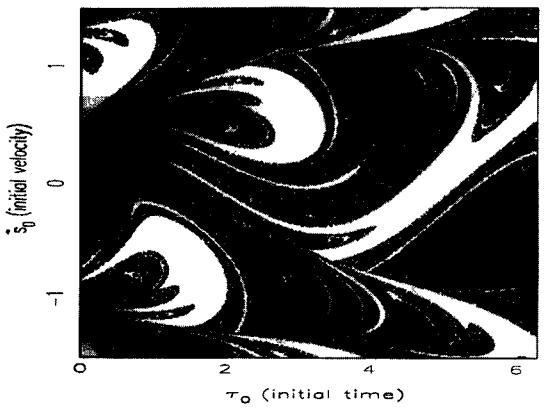

Figure 4. Basins of attraction of the two attractors shown in Figure 3. The gray and black basins correspond to the attractors A and B, respectively, in Figures 3a and 3b.

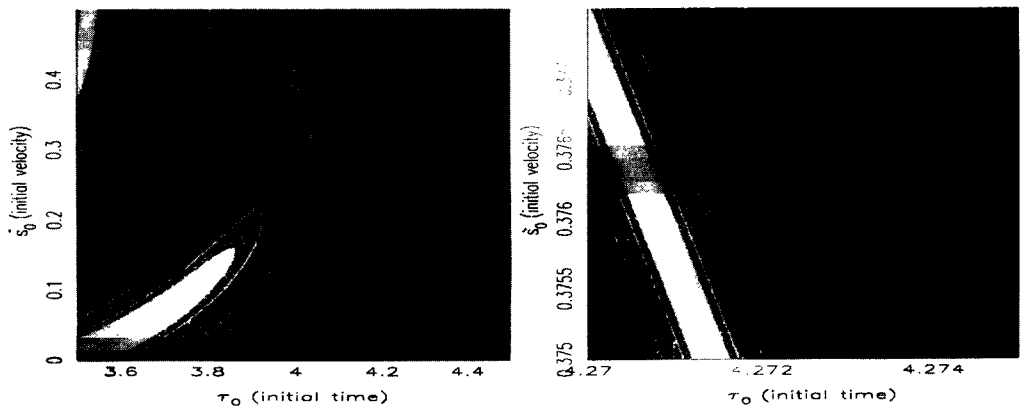

Figure 5. Successive magnifications of Figure 4.

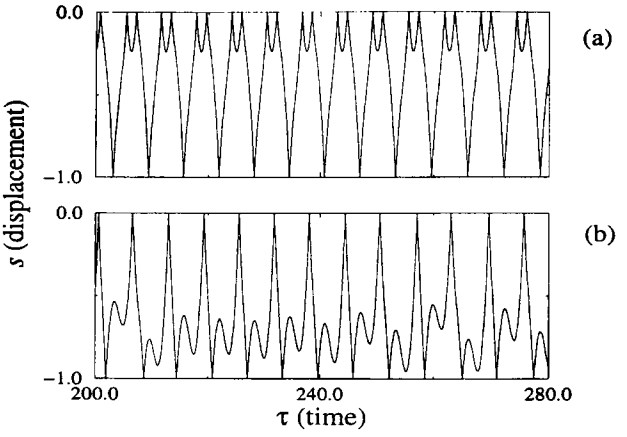

Figure 6. Displacement s as a function of time for the two coexisting periodic and chaotic attractors A (a) and B (b), respectively. Control parameter $\alpha = 0.57$.

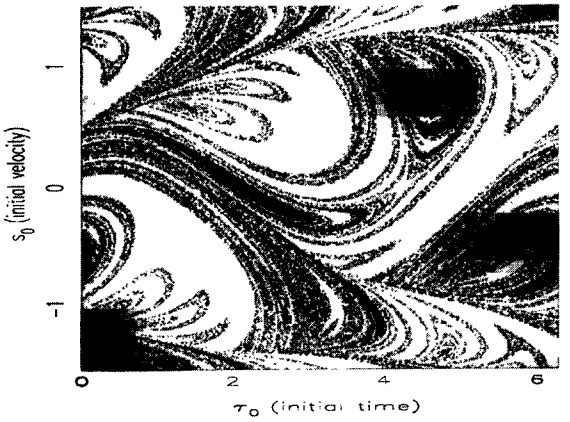

Figure 7. Basins of attraction of the two attractors shown in Figure 6. The gray and black basins correspond to the attractors A and B, respectively, in Figures 6a and 6b.

As a consequence of attractors' coexistence, what is seen in the bifurcation diagram as a bifurcation parameter is gradually changed for different initial conditions. Thus, the final state that is eventually reached depends on the initial state of the system. Next, we show that predictions of final states depend sensitively on the initial conditions.

For $\alpha = 0.48$, Figure 3 shows the time evolution of the relative displacement of the trajectories corresponding to the periodic attractors A and B of Figure 2. The corresponding basins of attraction of these attractors are shown in Figure 4. This figure is constructed using a grid of an equally spaced 400×400 set of initial condition points in the cross section $\dot{s}_0 \times \tau_0$ of the three-dimensional phase space. For trajectories starting at a point in this set, the limiting attractor is determined. The gray and black colors mark the basins of the attractors A and B. Some regions of these basins have highly interleaved fractal boundaries. To show this characteristic, we present in Figure 5 two successive magnifications of Figure 4. Figure 5 shows the coexistence of the two attractors and fine structures at any phase space scale. Consequently, there are regions for which the system's behavior is strongly dependent on small changes of initial conditions. However, there are other regions (Figure 4), or basin cells (Nusse and Yorke, 2000), for which the trajectory goes to only one attractor.

Figures 4 and 7 show the changes in the basins of attractors A and B as the bifurcation parameter increases from $\alpha = 0.48$ to $\alpha = 0.57$. In addition to that, Figures 3 and 6 show, for the same α values, the variation in time of the relative displacements of these attractors. For $\alpha = 0.48$, attractor B is periodic, but for $\alpha = 0.57$, it is chaotic due to a sequence of period-doubling bifurcations in this α interval. Comparing Figures 4 and 7, we see that the basin of attractor B (in black) decreases in size for increasing α. This happens until the chaotic attractor disappears for a specific α value, as we can see in the bifurcation diagram of Figure 2.

4. TRANSIENT CHAOS

In this section, we study chaotic transients and their dependence on the control parameter and initial conditions. We illustrate our conclusions with a case wherein, at a critical control parameter value, $\alpha_c \approx 1.2347058$, a chaotic attractor is converted into a chaotic transient that goes to a periodic attractor. The excitation amplitude, α, is the chosen control parameter. The results presented are obtained by varying α in the range [1.00, 1.75] and fixing the other system parameters in the usual following values: $\beta = 0.10, \gamma = 0.10$, and $r = 0.90$ (Karagiannis and Pfeiffer, 1991).

Figure 8a shows a bifurcation diagram of the system, namely, the relative velocity just before each impact, $\dot{s}_n$, as a function of the excitation amplitude α. In this figure, we identify only one dominant attractor that is periodic or chaotic, depending on α values, as indicated by the corresponding Lyapunov exponent values (calculated by using equation 11) shown in Figure 8b.

All the following figures of this work are calculated to investigate a crisis at which a chaotic attractor collapses and a periodic attractor appears for a critical parameter, $\alpha_c \approx 1.2347058$, as indicated in Figure 8a. Thus, Figure 9 shows the attractors before and after this crisis at $\alpha = \alpha_c$. The chaotic attractor for an α value smaller than the critical value is in Figure 9a. Gradually increasing the control parameter up to the critical value, its shape varies only slightly from that shown in this figure. The periodic attractor and its chaotic transient,

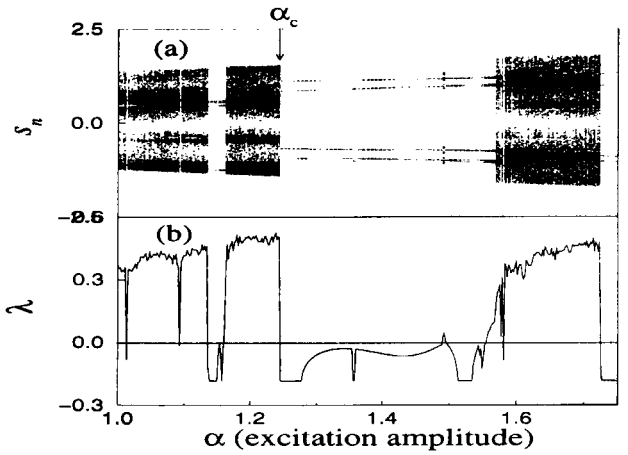

Figure 8. (a) Bifurcation diagram of the velocity $\dot{s}_n$ (just before impact) as a function of the excitation amplitude α, after transient of 5,000 iterates. (b) Largest Lyapunov exponent for the attractor as a function of α.

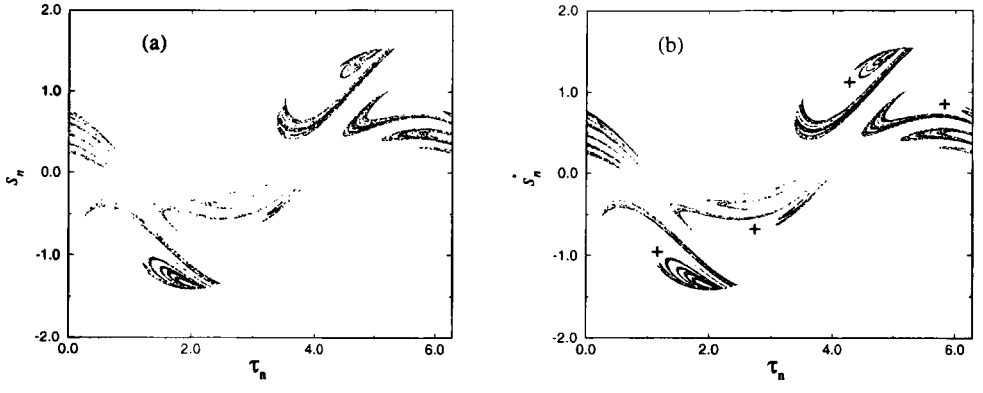

Figure 9. (a) Poincaré map of the chaotic attractor for $\alpha = 1.230 < \alpha_c$. (b) Poincaré map of the chaotic transient and periodic attractor (+) for $\alpha = 1.244 > \alpha_c$.

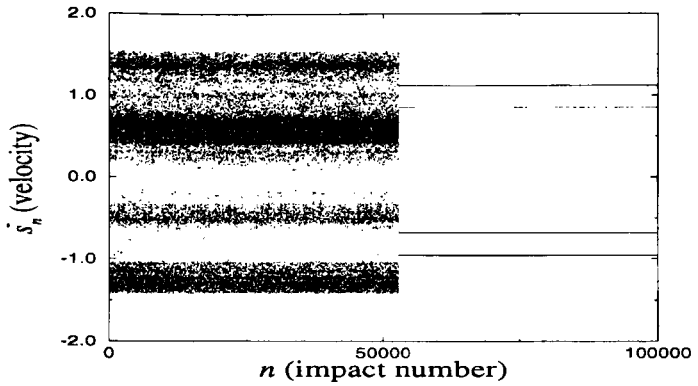

Figure 10. Evolution of relative velocity $\dot{s}_n$, just before each impact n, with a long chaotic transient, corresponding to Figure 9b.

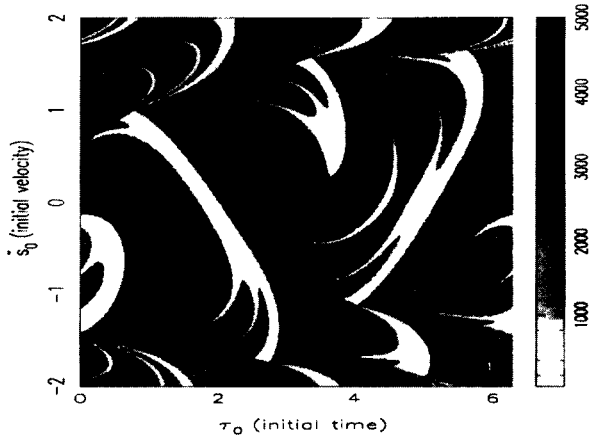

Figure 11. Lifetime calculated for a grid of 400×400 points corresponding to initial conditions in phase space. The grade scale indicates the number of impacts (transient) before the trajectory goes to the periodic attractor. Excitation amplitude $\alpha = 1.244 > \alpha_c$.

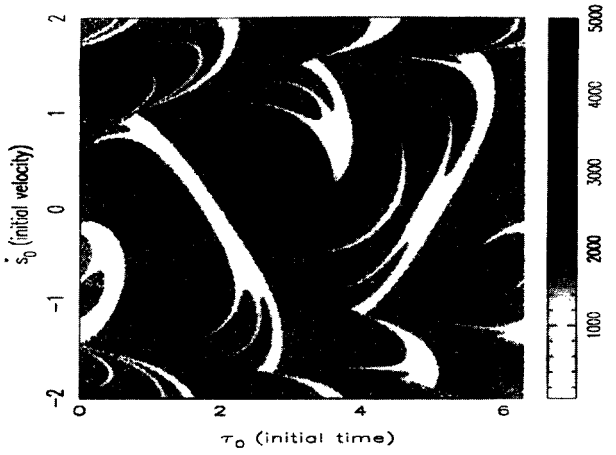

Figure 12. Lifetime calculated for a grid of 400×400 points corresponding to initial conditions in phase space. The grade scale indicates the number of impacts (transient) before the trajectory goes to the periodic attractor. Excitation amplitude $\alpha = 1.245 > \alpha_c$.

for a given initial condition and a parameter greater than the critical value, are in Figure 9b. As shown in these figures, the shape of the transient (in (b)) is similar to the previous collapsed attractor (in (a)). In addition, the lifetime of the transient shown in Figure 9b can be identified in Figure 10, which shows the evolution of relative velocity just before each impact as a function of the iterates.

For a fixed control parameter value, we present in Figure 11 the chaotic transient lifetime obtained for a set of initial conditions in a grid of points in a section of the three-dimensional phase space. The order of the transient lifetime depends strongly on the initial condition. In fact, there are continuous regions of initial conditions where this transient is very short (typically less than 100 iterates) and others with interleaved small regions of very short and very long transients (up to 100,000 iterates). Each calculated lifetime is marked with respect to a linear grade gray scale indicated in Figure 11. The white color indicates a very short lifetime, and the black color indicates a transient equal to 5,000 iterates or longer. Thus, most of the long transients are longer than 5,000 iterates and are represented by black marks in this figure.

Gradually increasing the control parameter, the area of the interleaved long transient regions decreases, consequently decreasing the average lifetime. This effect can be seen comparing Figure 11 with Figure 12. On the other hand, diminishing the control parameter, the white regions diminish and the average lifetime increases.

5. CONCLUSION

We use a gear-rattling model (Karagiannis and Pfeiffer, 1991) to numerically investigate basins of attraction of coexisting attractors, chaotic transients, and their dependence on the control parameters.

In summary, the structure of the bifurcation diagram shows that the system evolution switches from one attractor to another as the bifurcation parameter, the excitation amplitude, is slowly changed for different initial conditions. This shows how coexisting periodic and chaotic attractors are strongly dependent on small changes of the initial conditions. Moreover, the size and topology of the basins of attraction are modified by global bifurcations of their boundaries. Furthermore, for the considered control parameter range, the basin boundaries are fractals and so interleaved that the trajectory might deviate from one basin to another, due to small errors on the numerical simulations or noise in the system, causing jumps from one attractor to another (Okolewska and Kapitaniak, 1998). These trajectory deviations cause jumps, from one attractor to another, wherever we try to compute bifurcation diagrams following a specified attractor. These jumps should be observed experimentally and might affect the equipment safety and even the comfort.

Furthermore, we also investigate chaotic transients that occur as the amplitude excitation is varied past critical values following the sudden disappearance of the attractor. In these chaotic transients, orbits are attracted toward the vicinity of the former chaotic attractors and stay there for a large number of iterates. Then, suddenly, these orbits move off toward the periodic attractors. We conjecture that this is a boundary crisis, caused by a collision between the chaotic attractor and a coexisting unstable periodic orbit, like others that have been found in low-dimensional maps (Grebogi, Ott, and Yorke, 1983, 1986). Moreover, to illustrate our conclusions, we present an example of a chaotic attractor, corresponding to the gear oscillation, converted into a chaotic transient that goes to a periodic attractor, at a critical value of the excitation amplitude. Immediately following the crisis, the chaotic transient shape in phase space is similar to the chaotic attractor, and its lifetime depends sensitively on the initial conditions. For the considered control parameter range, this dependence is identified by structures of approximated equal lifetime formed on the initial conditions of phase space.

Acknowledgments. The authors thank Dr. Murilo S. Baptista and Dr. Kai Ullmann (University of São Paulo) for useful discussions. This work is partially supported by the Brazilian Government Agencies FAPESP, CAPES, and CNPq.

REFERENCES

Casas, F., Chin, W., Grebogi, C., and Ott, E., 1996, "Universal grazing bifurcations in impact oscillators," *Physical Review E* **53**, 134-139.

Grebogi, C., Ott, E., and Yorke, J. A., 1983, "Crises, sudden changes in chaotic attractors and transient chaos," *Physica D* **7**, 181-200.

Grebogi, C., Ott, E., and Yorke, J. A., 1986, "Critical exponent of chaotic transients in nonlinear dynamical systems," *Physical Review Letters* **57**, 1284-1287.

Grebogi, C., Ott, E., and Yorke, J. A., 1987, "Chaos, strange attractors, a fractal basin boundaries in nonlinear dynamics," *Science* **238**, 632-638.

Hinrichs, N., Oestreich, M., and Popp, K., 1997, "Dynamics of oscillators with impact and friction," *Chaos, Solitons, and Fractals* **8**(4), 535-558.

Kaharaman, A. and Singh, R., 1990, "Nonlinear dynamics of a spur gear pair," *Journal of Sound and Vibration* **142**, 49-75.

Karagiannis, K. and Pfeiffer, F., 1991, "Theoretical and experimental investigations of gear-rattling," *Nonlinear Dynamics* **2**, 367-387.

Li, G. X., Rand, R. H., and Moon, F. C., 1990, "Bifurcations and chaos in forced zero-stiffness impact oscillator," *International Journal Non-Linear Mechanics* **25**(4), 417-432.

Moon, F. C., 1998, *Applied Dynamics With Applications to Multibody and Mechatronic Systems*, John Wiley, New York.

Nordmark, A. B., 1991, "Non-periodic motion caused by grazing incidence in impact oscillator," *Journal of Sound and Vibration* **145**(2), 279-297.

Nusse, H. and Yorke, J. A., 2000, "Fractal basin boundaries generated by basin cells and the geometry of mixing chaotic flows," *Physical Review Letters* **84**, 626-629.

Okolewska, B. B. and Kapitaniak, T., 1998, "Co-existing attractors of impact oscillator," *Chaos, Solitons, and Fractals* **9**(8), 1439-1443.

Okolewska, B. B. and Peterka, F., 1998, "An investigation of the dynamic sys with impacts," *Chaos, Solitons, and Fractals* **9**(8), 1321-1338.

Peterka, F. and Vacik, J., 1992, "Transition to chaotic motion in mechanical systems with impacts," *Journal of Sound and Vibration* **154**, 95-115.

Pfeiffer, F., 1988, "Seltsame Attraktoren in Zahnradgetrieben," *Ingenieur Archiv* **58**, 113-125.

Pfeiffer, F. and Kunert, A., 1990, "Rattling models from deterministic to stochastic processes," *Nonlinear Dynamics* **1**, 63-74.

Thompson, J.M.T., 1996, "Global dynamics oscillators: Fractal basins and intermediate bifurcations," in *Nonlinear Mathematics and Its Applications*, P. J. Aston, ed., pp. 1-47, Cambridge University Press, Cambridge, UK.

Win, W., Ott, E., Nusse, H. E., and Grebogi, C., 1995, "Universal behavior of impact oscillators near grazing incidence," *Physics Letters A* **201**, 197-204.